Synthesis and characterization of chitosan-coated magnetite nanoparticles and their

application in curcumin drug delivery

Synthesis and characterization of chitosan-coated magnetite nanoparticles and their application in curcumin drug delivery

Xuan Nui Pham[1], Tan Phuoc Nguyen[1], Tuyet Nhung Pham[1], Thi Thuy Nga Tran[1] and Thi Van Thi Tran[2]

[1] Department of Chemical Engineering, Hanoi University of Mining and Geology, 18 Pho Vien, Duc Thang, Bac Tu Liem district, Hanoi, Vietnam
[2] Department of Chemistry, Hue Science College, Hue University, 77 Nguyen Hue Street, Hue City, Vietnam

E-mail: phamxuannui@gmail.com

CrossMark

Abstract

In this work anti-cancer drug curcumin-loaded superparamagnetic iron oxide (Fe_3O_4) nanoparticles was modified by chitosan (CS). The magnetic iron oxide nanoparticles were synthesized by using reverse micro-emulsion (water-in-oil) method. The magnetic nanoparticles without loaded drug and drug-loaded magnetic nanoparticles were characterized by XRD, FTIR, TG-DTA, SEM, TEM, and VSM techniques. These nanoparticles have almost spherical shape and their diameter varies from 8 nm to 17 nm. Measurement of VSM at room temperature showed that iron oxide nanoparticles have superparamagnetic properties. *In vitro* drug loading and release behavior of curcumin drug-loaded CS-Fe_3O_4 nanoparticles were studied by using UV-spectrophotometer. In addition, the cytotoxicity of the modified nanoparticles has shown anticancer activity against A549 cell with IC_{50} value of 73.03 $\mu g/ml$. Therefore, the modified magnetic nanoparticles can be used as drug delivery carriers on target in the treatment of cancer cells.

Keywords: curcumin (Cur), chitosan (CS), magnetic nanoparticles (Fe_3O_4), nanoparticles, *in vitro* cytotoxicity

Classification number: 5.02

1. Introduction

Chemotherapy is not specialized to a certain treatment, which is the most notable drawback of this therapy method. When drug goes into the body, the medicine does not concentrate mainly on the diseased cells. Hence, magnetic particles are recently used to carry the drugs to the required location in the body, typically cancer tissues. The method of using superparamagnetic iron oxide nanoparticles has received much attention from the research community with two main objectives: (i) to narrow the distribution of drugs in the body for reducing the side effects; (ii) to reduce the amount of drug consumption.

The biocompatible magnetic nanoparticles are encapsulated with drugs. They work as drug delivery carriers and control the drug release process. Therefore, the application of superparamagnetic iron oxide nanoparticles in diagnosis and therapeutics has gained many promising achievements such as cell separation [1], cell apoptosis [2], and enzyme immobilisation [3]. Generally, the drug–particle system creates a magnetic liquid and enters the body via the circulatory system. When the particles enter the blood vessel, a strong external magnetic field gradient is used to guide the particles to arrive at the targeted location in the body. When the drug–particle system is concentrated at the required location, the

drug release process is taken place by enzyme activity or physiological property change of cancer cells causing the variation of pH, diffusion, and temperature. Drug carried by magnetic nanoparticles can easily be directed to a targeted location in the body by magnetic force [4, 5]. Meanwhile, the polymer coated drug can delay the releasing speed. Therefore, the magnetic nanoparticles coated polymer system are considered to be an effective method to target the cancer cells.

The magnetic material is iron oxide covered by organic or inorganic molecules which form chemical bonds with the surface of Fe_3O_4 nanoparticles. Iron oxide core particles are nanometer-size superparamagnetic particles. Modified magnetic nanoparticles have been studied by different researchers [6, 7] using 3-aminopropyl triethoxy silane (APTES) coated by nano-carrier through adsorption or covalent bond creating active amino groups to carry anti-cancer drugs. Yao *et al* [8] prepared magnetic Fe_3O_4/SiO_2-GO core/shell nanoparticles by means of covalent and used as adsorbent. Their results show that this material has a relatively high adsorption ability. In another study, Peng *et al* [9] reported a simple method to synthesize mesoporous nanoparticles of core–shell structure Fe_3O_4-@mZnO to use as drug delivery carriers.

Curcumin, an anti-cancer drug, is derived from phenol which is connected by two α, β-unsaturated carbonyl groups. The diketones form stable enols and are readily deprotonated to form enolates. The α, β-unsaturated carbonyl group is a good michael acceptor and undergoes nucleophilic addition. Therefore, they are biologically characterized as antioxidant [10], anti-inflammatory [11], antibacterial [12], and antitumor activity [13]. However, solubility of curcumin in water is low, unstable and the short half-life cycles of *in vitro* metabolism limited its clinical application. To increase the solubility in water and biological compatibility of curcumin, different carriers were tested to encapsulate drug in polymer micelles [14], solid-lipid particles [15], and nano-polymeric particles [16].

Among the available polymers, natural chitosan shows some promising results in drug delivery system. Chitosan (CS), the second most naturally abundant polymer after cellulose, is a natural bio-polymer derived from alkaline deacetylation of chitin. Due to its chemical structure and the non-toxic nature [17], CS has received much attention and used widely in many fields such as adsorbent [18] and anti-bacterial membrane [19]. In some recent applications, CS is often used in drug delivery system [20–22] and protein carriers [23].

Many different methods have been investigated to synthesize magnetic nanoparticles such as co-precipitation, sol-gel process, micro-emulsion, ultrasonic chemistry, hydrothermal, hydrolysis, thermolysis, and flow injection method. The formation of nanoparticles depends on the synthetic method. Micro-emulsion method has high capability to disperse Fe_3O_4 nanoparticles in a solution and particle size can be well controlled by the surfactant.

In this study, superparamagnetic Fe_3O_4 nanoparticles were synthesized by micro-emulsion method used as carriers.

The carrier was coated as chitosan to create a polymeric shell to form an active amino group on its surface to be able to combine with the anti-cancer curcumin (Cur) drug. The morphology, structure, and characteristic of iron oxide nanoparticles coated with CS solution were studied by x-ray diffraction (XRD), Fourier transform infrared spectroscopy (FTIR), scanning electron microscopy (SEM), transmission electron microscopy (TEM), thermogravimetric analysis (TGA), differential thermal analysis (DTA), and vibrating sample magnetometer (VSM). The application of chitosan-loaded magnetic nanoparticles (CS-MNPs) as carrier of Cur was evaluated by loading and releasing profiles and *in vitro* cytotoxicty.

2. Experimental

2.1. Materials

Iron (III) chloride hexahydrate ($FeCl_3.6H_2O$), iron (II) sulfate heptahydrate ($FeSO_4.7H_2O$), ammonium hydroxide (28% w/w NH_3), chitosan ($C_6H_{11}NO_4$)$_n$ with deacetylation degree of 86%, MW = 60 kDa, glass acetic acid, butanol (C_4H_9OH), tween-80, heptane, cetyl trimethylammonium bromide (CTAB), and curcumin were purchased from E-Merck Products. All other reagents were analytical grade and used directly without any purification, and A549 (human lung carcinoma cell line) cell was provided by the University of Milan, Italy.

2.2. Synthesis of magnetic Fe_3O_4 nanoparticles

The Fe_3O_4 magnetic nanoparticles were prepared by water-in-oil micro-emulsion method. The precursor solution (solution A) contains 2:1 mole ratio of iron salts (10 ml of 0.4 M $FeCl_3.6H_2O$ and 10 ml of 0.2 M $FeSO_4.7H_2O$) dissolved in 45 ml mixture of tween-80/butan-1-ol/n-heptane. This resulted in the formation of a reverse micro-emulsion. Mixture B contains 45 ml of tween-80/butan-1-ol/n-heptane added to aqueous NH_3 (56 ml of 28% aqueous NH_3). These solutions were stirred with speed of 300 rmp/min for 30 min at room temperature. Mixture B was added to solution A and the combined mixture was stirred continuously with a rotational speed of 1000 rpm for 24 h at different temperatures were 30, 50, and 80 °C. Formed magnetic nanoparticles were separated by magnetic force and washed several times by distilled water to eliminate the ammonia. Finally, the magnetic Fe_3O_4 nanoparticles were obtained after drying in a vacuum oven, and recorded as Fe_3O_4-30, Fe_3O_4-50, and Fe_3O_4-80, respectively.

2.3. Synthesis of chitosan-coated magnetic Fe_3O_4 nanoparticles

The surface of magnetic Fe_3O_4 nanoparticles was coated with a solution of CS for the purpose of obtaining modified magnetic nanoparticles. In a typical experiment, 0.25 g of magnetic Fe_3O_4 nanoparticles was dispersed in a surfactant

Adv. Nat. Sci.: Nanosci. Nanotechnol. **7** (2016) 045010

X N Pham *et al*

containing CTAB (2 grams of CTAB dissolved in 400 ml of deionized water) (solution C). Then, 100 ml chitosan solution (0.02 gram CS powders dissolved in 100 ml of 1% (w/v) acetic acid solution) was slowly dropped into solution C. The mixture was continuously stirred with a rotational speed of 1000 rpm for 1 h at room temperature. Then, CS coated by magnetite nanoparticles was magnetically separated from solution by a magnet bar and thoroughly washed several times with ethanol and deionized water. Finally, the obtained nanoparticles were dried overnight at 60 °C.

2.4. Characteristics of materials

Powder x-ray diffraction patterns were recorded on a D8-Advance Bruker with Cu-Kα radiation ($\lambda = 1.5406$ nm). Morphological analysis was examined on a Hitachi S-4800 scanning electron microscope (SEM). The images of TEM were taken by a JEM-1010 (Jeol, Japan) operated at an accelerating voltage of 200 kV. Infrared data were examined on KBr pallets by using a Shimadzu IR Prestige-21 spectrometer (Japan). TGA and DTA were performed with a TG Setaraminstrument (France) in the air of argon (100–1000 °C). The magnetization of the prepared nanoparticles was measured on a VSM (DMS-88) at room temperature.

UV–vis and UV–vis-diffuse reflectance spectra were collected on a DR–Jasco V630 or a UV–vis DRS–Jasco V670 spectrophotometer that was equipped with a diffuse reflectance attachment in which BaSO$_4$ was the reference.

2.5. In vitro curcumin drug loading and release experiments

Anti-cancer curcumin drug was loaded on magnetic Fe$_3$O$_4$ nanoparticles coated by chitosan (CS). Loading of curcumin was performed by dispersing 0.3 gram of chitosan-coated magnetic Fe$_3$O$_4$ nanoparticles (CS-Fe$_3$O$_4$) nanoparticle in 0.1% curcumin solution (dissolved in ethanol) and stirred for 3 h to increase the uptake of curcumin. At each fixed period of time, the magnetic nanoparticles were separated from the mixture by using a magnet. The absorbance of the residual curcumin in the supernatant was measured at $\lambda_{max} = 428$ nm by UV–vis spectrophotometer to determine the drug concentration of curcumin. The curcumin loading was determined from the difference between the initial concentration of curcumin in solution and concentration of curcumin in the supernatant solution after the set time interval.

The release profile of the curcumin drug studied in phosphate buffered saline (PBS) at pH of 7.4. 0.3 g of Cur-CS-Fe$_3$O$_4$ was dispersed in PBS at 37 °C and shaking slightly at a rate of 150 cycles/min. At each time intervals, the concentration of curcumin release in the PBS was analyzed by UV–vis spectrophotometer.

2.6. In vitro cytotoxicity assay

A549 cancer cell lines were cultured as monolayers in the culture medium of Dulbecco's modified eagle medium
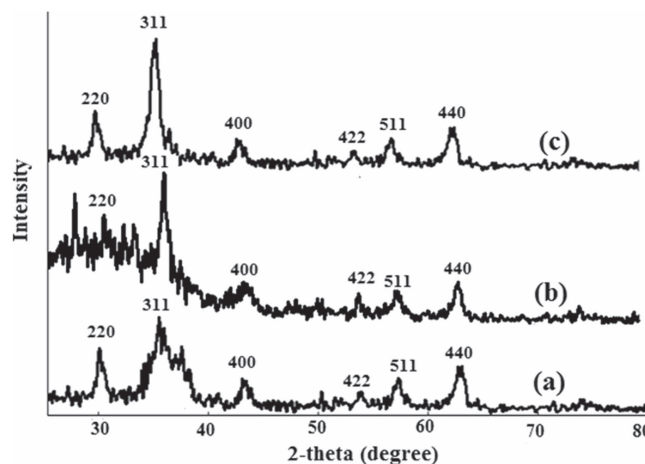

Figure 1. XRD patterns of (a) magnetic Fe$_3$O$_4$-30, (b) Fe$_3$O$_4$-50 and (c) Fe$_3$O$_4$-80 nanoparticles.

(DMEM) along with other components including 2 mM L-glutamine, 10 mM 4-(2-hydroxyethyl)-1-piperazineethanesulfonic acid (HEPES), and 1.0 mM sodium pyruvate. 10% fetal bovine serum (FBS, Gibco) was also added. The cells were cultured and moved after 3–5 days with a ratio of 1:3 and cultured in CO$_2$ incubator at 37 °C with 5% CO$_2$. Monks's method [24] was implemented for vitro cytotoxicity. The test was conducted to determine the amount of total cell protein based on the optical density (OD) measured the protein components of the cell stained with the sulforhodamine B (SRB). 20 μl of the A549 cells diluted in 10% of dimethyl sulfoxide (DMSO) was put into the standard 96-well plates to obtain different concentrations of 100 μg ml^{-1}, 20 μg ml^{-1}, 4 μg ml^{-1}, and 0.8 μg ml^{-1}. Trypsinized cells were used to separate and count cells in the counting chamber to obtain a suitable experimental density. A suitable number of cells was added to the wells (in 180 ml medium) and so they can develop within 3–5 days. Other 96-well plates without the A549 cells containing 180 μl cancer cells were used to control day 0. After 1 h, the cells in the control plate of day 0 were immobilized by trichloracetic acid (TCA). After a period of development in the CO$_2$ incubator, the cells were immobilized to the bottom of the well by TCA and stained by SRB in 1 h at 37 °C. After removing the SRB, the experimental wells were washed 3 times with acetic acid and dried by air at room temperature.

Finally, 10 mM unbuffered tris base was used to dissolve the SRB sticking on the protein molecules. The system was put on a shaker plate shaking gently for 10 min Then, elisa plate reader (bio-rad) was used to read the color content of the SRB through UV–vis at $\lambda_{max} = 540$ nm. The cell viability (%) was related to the control wells containing untreated cells with fresh cell culture medium. The cell viability was calculated by the following formula:

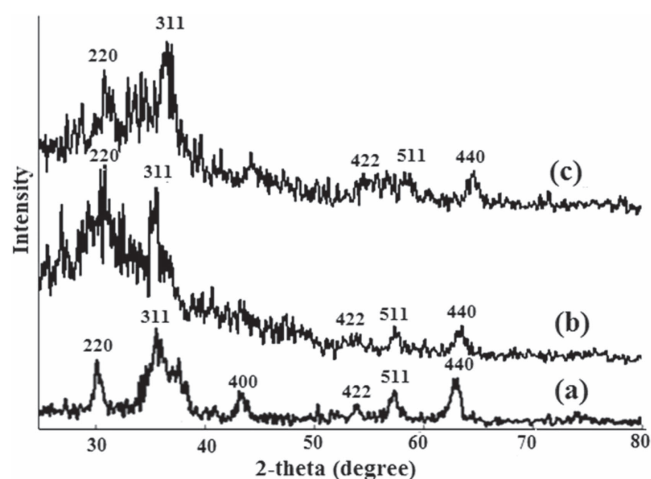$$Cell\ viability\ (\%) = \frac{Absorption\ test}{Absorption\ control} \times 100.$$

Figure 2. XRD patterns of (a) uncoated Fe₃O₄, (b) CS-Fe₃O₄ and (c) Cur-CS-Fe₃O₄ nanoparticles.

Figure 3. FTIR spectra of (a) uncoated Fe₃O₄, (b) chitosan coated Fe₃O₄ (CS-Fe₃O₄) and (c) curcumin loaded CS-Fe₃O₄ nanoparticles.

3. Results and discussion

3.1. Characterization of prepared nanoparticles

3.1.1. X-ray diffraction. Figure 1 shows the results of x-ray diffraction (XRD) analysis for magnetic iron oxide nanoparticles synthesized by micro-emulsion method at different temperatures (30 °C, 50 °C and 80 °C). The Fe₃O₄ diffraction patterns have six main peaks at 2θ values of 30.1°, 35.5°, 43.2°, 53.5°, 57°, and 62.8° corresponding to the reflection from (220), (311), (400), (422), (511), and (440) crystal planes. Positions and relative intensities of all the peaks are in accordance with the cubic crystalline system of Fe₃O₄ nanoparticles. Patterns of iron oxides and oxyhydroxide products of the JCPDS card. no. 79-0418 database were included for comparison. The narrow shape peaks of materials indicate that the nanoparticles have relatively high crystallinity, and without the appearance of the impurities phase of goethite α-FeO(OH) and hematite (Fe₂O₃) corresponding to the diffraction peaks of (110), (104) at 2θ positions of 21.22° and 33.15°.

Broadness of the diffraction peaks was related to particle sizes. Scherrer's equation

$$D = \frac{k\lambda}{\beta \cos \theta}$$

was used to calculate the average particle size D. In this equation θ is the angle of the peak, β is the full width at half maximum (FWHM) of the respective XRD peak, λ is the x-ray radiation wave-length in angstroms, and k is a constant. The broadening of Bragg's peaks indicates the formation of nanoparticles. The calculated mean crystallite size of the Fe₃O₄ nanoparticles synthesized by micro-emulsion method with three different temperatures 30 °C, 50 °C and 80 °C was about 8.5, 16.7 and 25 nm, respectively. The magnetic Fe₃O₄ nanoparticles synthesized at 30 °C is used for further studies.

The XRD analysis results for samples of magnetic Fe₃O₄ nanoparticles coated by chitosan (CS-Fe₃O₄) and CS-Fe₃O₄

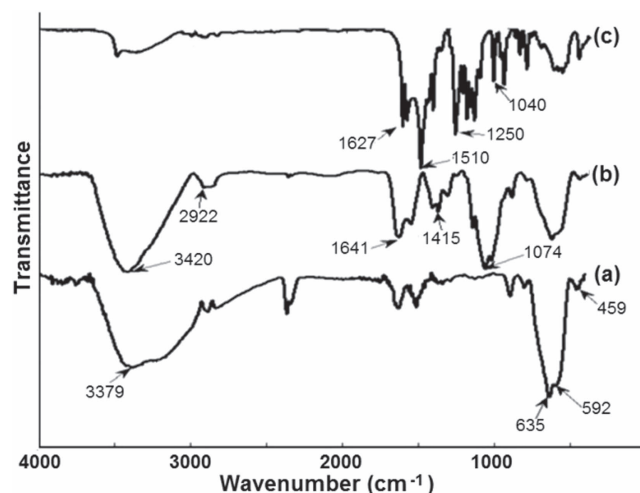loaded by curcumin (curves b and c in figure 2, respectively) showed characteristic peaks for Fe₃O₄ corresponding to the crystal planes of (220), (311), (422), (511), (440), which revealed that after surface modification, nanoparticles were pure Fe₃O₄ with a cubic structure.

3.1.2. FTIR spectra analysis. FTIR was performed to confirm the functional groups on surface of the synthetic materials. The spectra of pure Fe₃O₄, CS-Fe₃O₄ and Cur-CS-Fe₃O₄ were shown in figure 3. The presence of two strong absorption bands of all materials at around 636 and 592 cm⁻¹ shows the formation of magnetic nanoparticles. Moreover, the band at 592 cm⁻¹ was confirmed as the Fe-O stretching vibration of tetrahedral sites of spinel structure [25]. The absorption bands at 459 cm⁻¹, attributed to tetrahedral and octahedral sites [26], peaks at 3400 cm⁻¹ due to the O-H stretching model adsorbed on the surface of the Fe₃O₄ nanoparticles [27].

In the case of CS coated magnetic Fe₃O₄ nanoparticles (curve b in figure 3), the coating of CS is established by the appearance of the peak at 2922 cm⁻¹ considered to be the stretching vibrations of –CH– in chitosan. The peak at 1641 cm⁻¹ is relevant to the N–H vibration for the chitosan. In addition, the C-N vibration of amino group is at 1415 cm⁻¹ and the C–O in the ether group is at 1074 cm⁻¹. The comparison of the spectra of Cur-CS-Fe₃O₄ with those of CS-Fe₃O₄ and Fe₃O₄, shows that the peak at 1510 cm⁻¹ and the band at 1627 cm⁻¹ is attributed to the C–C stretching vibration of the aromatic ring. This indicates the presence of aromatic CH bending vibration.

On the other hand, the appearance of two strong bands at about 1250 and 1040 cm⁻¹ (curve c in figure 3) was confirmed as vibration of methyl phenyl ether group (C-O-CH₃) [28]. This suggests that curcumin binds very strongly with chitosan coated magnetic Fe₃O₄ nanoparticles.

3.1.3. Scanning electron microscopy and transmission electron microscopy analysis. Morphological analysis was studied
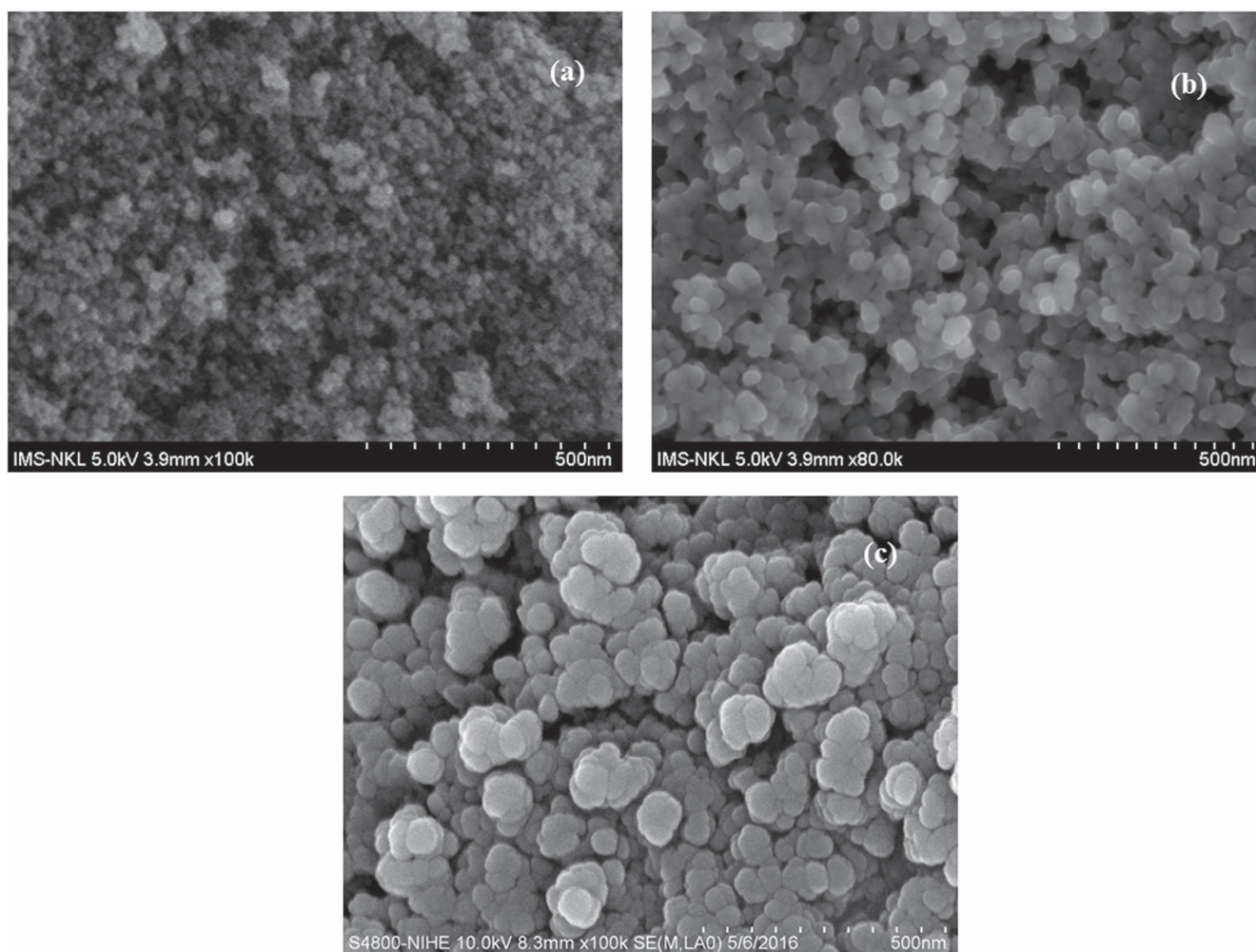
Adv. Nat. Sci.: Nanosci. Nanotechnol. **7** (2016) 045010

X N Pham *et al*

Figure 4. SEM micrographs of (a) Fe$_3$O$_4$-30; (b) Fe$_3$O$_4$-50; và (c) Fe$_3$O$_4$-80 nanoparticles.

with electron microscopic images. In the SEM images of Fe$_3$O$_4$ nanoparticles, it can be seen clearly that the particles are uniformly aggregated, spherical shaped with size 8–25 nm (figure 4).

SEM images of magnetic uncoated-Fe$_3$O$_4$ nanoparticles, CS-coated Fe$_3$O$_4$ (CS-Fe$_3$O$_4$) nanoparticles and Cur-loaded CS-Fe$_3$O$_4$ are shown in figure 5. The results suggested that all nanoparticles are most spherical in shape and the size of the CS coated Fe$_3$O$_4$, and curcumin-loaded CS-Fe$_3$O$_4$ nanoparticles was in the range from 8–17 nm. From these results, it may prove indirectly that the magnetic core/shell particles remain single crystals to have an average diameter of 8 nm, and the polymer shells have the approximate thickness of 9 nm. The results suggest that the polymer layer is uniformly deposited on Fe$_3$O$_4$ nanoparticles, as shown in figures 5(b) and (c).

The TEM images in figure 6 of CS-Fe$_3$O$_4$ and Cur-CS-Fe$_3$O$_4$ nanoparticles reveal that the magnetic nanoparticles are spherical in shape, and the average size was 13–17 nm. Thus, the immobilized polymer on nanoparticles did not lead to the aggregation between the particles. This shows the appearance of the bonds on surface of magnetic Fe$_3$O$_4$ nanoparticles.

3.1.4. Thermogravimetry differential thermal analysis analysis. The thermal properties of Fe$_3$O$_4$, CS-Fe$_3$O$_4$ and Cur-CS-Fe$_3$O$_4$ were investigated by analytical techniques of TG-DTA. Measurement is conducted under air atmosphere at a heating rate of 10 °C min^{-1} up to 800 °C. The unloaded Fe$_3$O$_4$ nanoparticles have the initial weight loss of 5.2% in the range of 30–220 °C (curves a in figures 7(A) and (B)). This stage may be the evaporation of water or OH groups adsorbed on the surface of the iron oxide. In the second stage, the weight loss of 3.7% corresponds to the broad exothermic peak at 235 °C (curves b in figures 7(A) and (B)). The cause of this occurrence is due to the oxidation products of Fe$_3$O$_4$ that are easily oxidized to give γ-Fe$_2$O$_3$ particles [29].

The weight loss of 12.7% corresponds to the strong exothermic peak at 433 °C (curves c in figures 7(A) and (B)). This shows that the OH groups on the surface of the magnetic nanoparticles are covalently bonded to the NH$_2$ groups in chitosan molecules. Hence, it could infer that the weight loss was the release of hydroxyl ions and decomposition of chitosan on the Fe$_3$O$_4$ nanoparticles except water thermo-desorption. It was also confirmed that the Fe$_3$O$_4$ nanoparticles were successfully coated by chitosan. In addition, the sharp
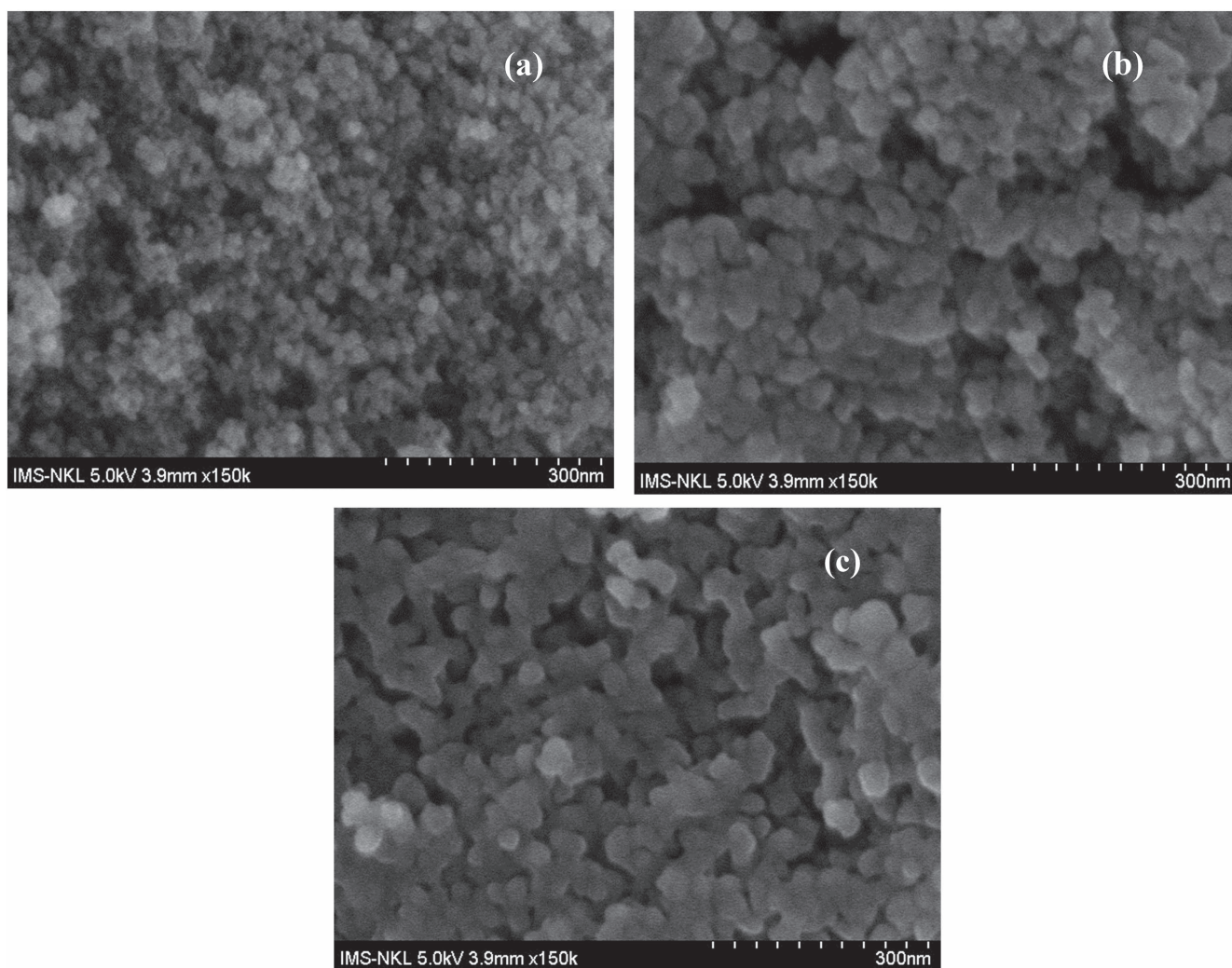
Figure 5. SEM images of (a) uncoated Fe_3O_4, (b) CS-Fe_3O_4 and (c) Cur-CS-Fe_3O_4 nanoparticles.

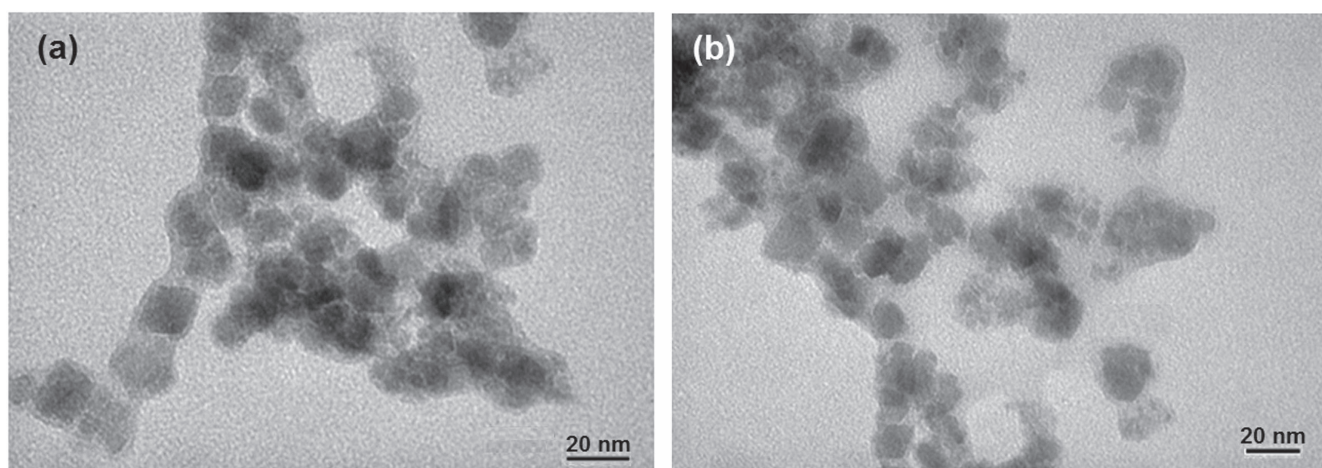**Figure 6.** TEM images of (a) CS-Fe_3O_4, and (b) Cur-CS-Fe_3O_4 nanoparticles.

weight loss of 55.1% corresponding to the exothermic peak at 491 °C confirmed the decomposition of carbon skeleton and hydroxyl groups in molecule of curcumin loaded on surface of magnetic CS-Fe_3O_4 nanoparticles.

3.1.5. Magnetic properties. The magnetization curves of magnetic nanoparticles of Fe_3O_4, CS-Fe_3O_4 and Cur-CS-Fe_3O_4 are given in figure 8. As shown in figure 8, the zero coercivity (Hc = 0) and magnetic remanence (Mr = 0) are

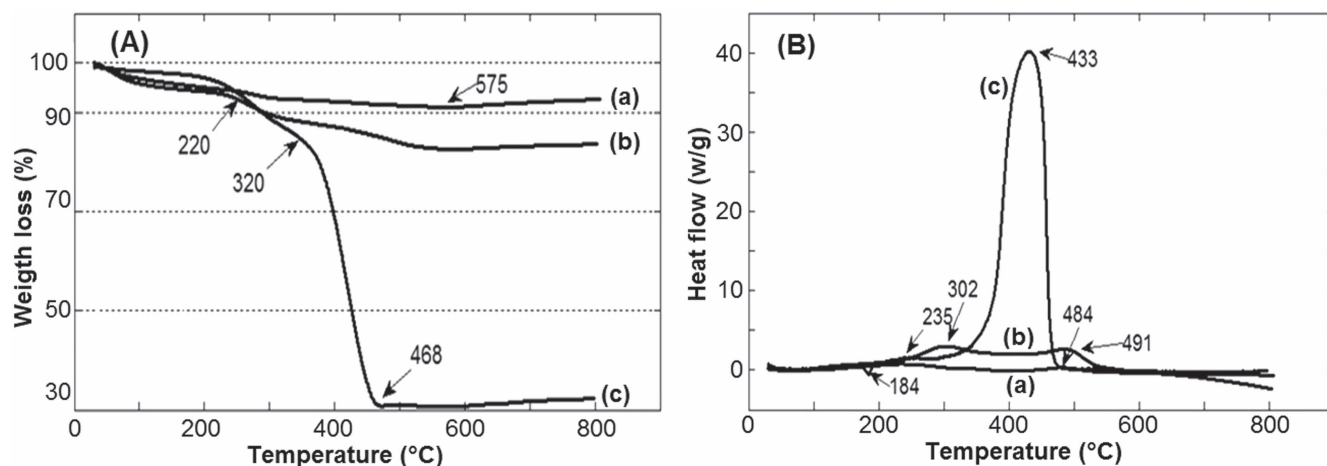**Figure 7.** (A) TGA curves and (B) DTA curves for (a) uncoated Fe_3O_4, (b) CS-Fe_3O_4 and (c) Cur-CS-Fe_3O_4 nanoparticles.

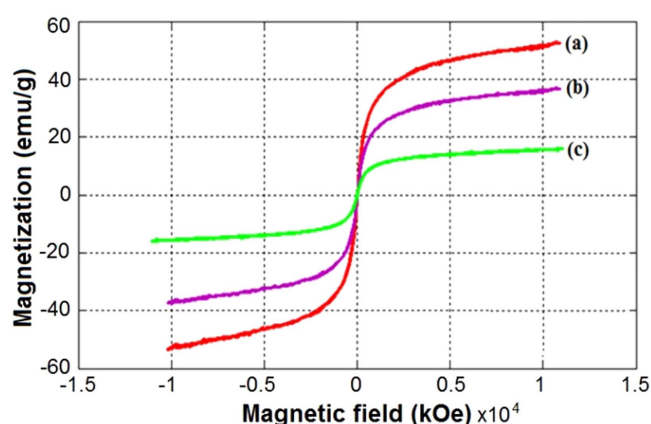**Figure 8.** VSM magnetization curves of (a) uncoated Fe_3O_4, (b) CS-Fe_3O_4, and (c) Cur-CS-Fe_3O_4 nanoparticles.

observed in all of the magnetic hysteresis curves, which suggest that synthetic materials have superparamagnetic properties. The saturation magnetization (Ms) values of the magnetic Fe_3O_4, CS-Fe_3O_4 and Cur-CS-Fe_3O_4 nanoparticles were 90 emu g^{-1} and 50 emu g^{-1} and 18 emu g^{-1}, respectively. The decrease in Ms values of CS-Fe_3O_4 and Cur-CS-Fe_3O_4 compared to that of magnetic uncoated Fe_3O_4 nanoparticle is due to the decrease in particles size. Along with that, the particle size increase is due to the polymer layer coated on the surface of the particles and this also leads to a decrease in the value of magnetic saturation.

The results of vibrating sample magnetometer (VSM) show that all particles have superparamagnetic properties at room temperature since the zero coercivity and the remanence are almost negligible in the absence of an external magnetic field. According to the study by Mohapatra *et al* [30], Yavuz *et al* [31], superparamagnetism exhibited in the nanopaticles is due to their size effect (<50 nm). The average particle diameter of prepared samples is smaller than the critical size of superparamatic Fe_3O_4 at room temperature. The Fe_3O_4 particles are considered to be at their superparamagnitism. On the other hand, it is considered that the superparamagnetic

properties may also be due to the high crystallinity of the prepared spherical shape magnetic nanoparticles.

3.1.6. In vitro drug loading and release studies. Figures 9 and 10 represent the *in vitro* drug loading and release profile of curcumin from Cur-CS-Fe_3O_4 nanoparticles. The loading profile (figure 9(b)) shows the rapid adsorption of curcumin in the initial stages and the adsorption rate slowed down after 90 min Because the surface of the nanoparticles is incorporated by curcumin, the final saturation point was reached at 120 min. In addition, the adsorption time of 120 min did not significantly change the concentrations of curcumin because curcumin with the nanoparticles had reached the saturation point. From the results obtained above, it can be concluded that the maximum drug absorption time is short, about 120 min.

Figure 10 depicts the *in vitro* drug release profile of curcumin from Cur-CS-Fe_3O_4 nanoparticles at the pH of 7.4 and the release in phosphate buffer solution, at 37 °C.

The UV-spectra of curcumin loaded CS-Fe_3O_4 nanoparticles dissolved in buffer show an increase in absorbance with the increase in time. However, the release rate is relatively slow when the time was prolonged. The drug release rapidly occurs for the first 180 min. This may be due to the excess of curcumin drug molecules dispersed from matrix of the magnetic nanoparticles into buffer solutions, leading to the drug release at a faster rate [32]. The slow drug release was attributed to the presence of highly soluble phenolic acid groups in ionized drugs and the concentration reduction of chitosan on the surface [33].

About 30% of the un-released curcumin remining on the magnetic nanoparticles matrix for 2800 min may be due to inter-molecular hydrogen bonding of curcumin and also because chitosan has hindered the drug release from the particles [34, 35]. This result is similar to that of the previous study by Ramanujan *et al* [34]. Drug loading and release profiles of PVA coated iron oxide nanoparticles showed that up to 45% of adsorbed drug was released in 80 h. Thus, the results show that Cur-loaded CS-coated iron oxide
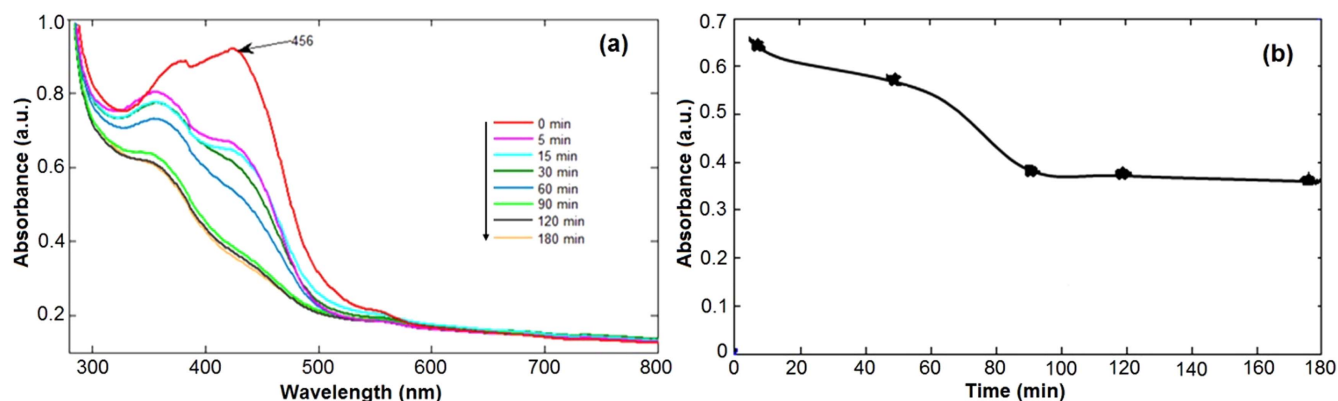
Figure 9. *In vitro* drug loading of curcumin on CS coated Fe_3O_4 nanoparticles: (a) absorption spectra and (b) absorption rate at different times.
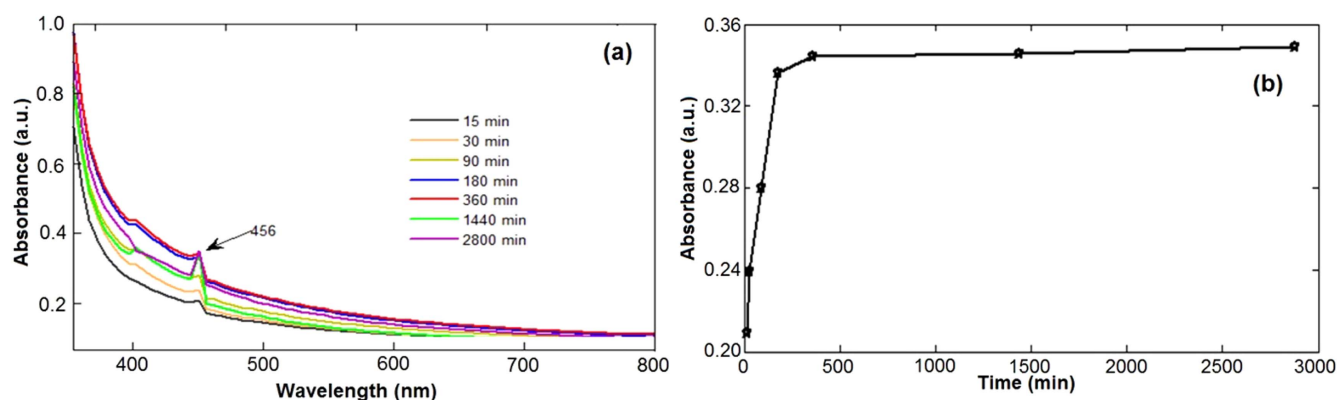

Figure 10. *In vitro* drug curcumin release from CS coated Fe_3O_4 nanoparticles in buffer with pH of 7.4: (a) absorption spectra and (b) absorption rate at different times.

Table 1. Cytotoxicity assay of free-curcumin and curcumin loaded CS-Fe_3O_4 nanoparticles.

A549 cell lines con-centration ($\mu g/ml$)	Sample	
	free Cur (% of inhibitions)	Cur-CS-Fe_3O_4 (% of inhibitions)
6.25	11.57	4.98
12.5	69.26	16.39
25	87.5	24.32
50	90.4	31.59
100	94.4	78.55
IC_{50}	11.37	73.03

nanoparticles are promising magnetic drug carriers to use in magnetically targeted drug delivery.

3.2. In vitro cytotoxicity assay

The cytotoxicity of free Cur and magnetic Cur-CS-Fe_3O_4 nanoparticles evaluated against A549 cell lines with the concentrations ranging from 6.25 $\mu g\,ml^{-1}$ to 100 $\mu g\,ml^{-1}$ is presented in table 1. It was observed that cell inhibition was decreased at lower concentrations of nanoparticles. That is due to the lower concentrations of drug loaded into

nanoparticles. The cancer cells treated with a lower con-centration (10 $\mu g\,ml^{-1}$) of the curcumin loaded magnetic Fe_3O_4 nanoparticles show a low percentage of inhibitions (4.98%) whereas curcumin loaded magnetic nanoparticles with higher concentrations (100 $\mu g\,ml^{-1}$) have a very high ability to inhibit cancer cells (78.55 $\mu g\,ml^{-1}$). With this concentration, the free-curcumin inhibited cancer cells were 94.4%. Because of the slower release rates of curcumin from nanoparticles, it reduces the interaction of the drug with a cell wall.

From the obtained results, table Curve software was used to calculate the IC_{50} values. IC_{50} is the drug concentration at which the drug includes 50% inhibition of the growth of the cells. The results obtained from the two samples of free-curcumin and magnetic Cur-CS-Fe_3O_4 nanoparticle shown the activity on cancer the A549 cell line with an IC_{50} value of 73.03 and 11.37 $\mu g\,ml^{-1}$, respectively. It suggests that chit-osan-coated magnetic nanoparticles have no cytotoxicity at the normal concentration and show a good biocompatibility.

4. Conclusions

Magnetic Fe_3O_4 nanoparticles are synthesized by a reverse micro-emulsion of water-in-oil. The synthesized magnetic

nanoparticles (MNPs) showed relatively small size and good magnetic responsivity. The magnetic carrier was formed by the chitosan-coated MNPs which were characterized by XRD, FTIR, SEM, TEM, TG/DTA, and VSM techniques. TEM results showed that the magnetic nanoparticles have spherical shaped morphology and the average size from 8 to 17 nm. The FTIR and TG/DTA data indicate that the functional groups were successfully attached on surface of the nano-particles. The outcomes of VSM proved that the un-coated Fe_3O_4, $CS\text{-}Fe_3O_4$ và $Cur\text{-}CS\text{-}Fe_3O_4$ nanoparticles have a superparamagnetic characteristic. The *in vitro* studies of Cur-loaded CS-coated showed up to 70% of adsorbed drug released in the buffer solution after 2800 min The *in vitro* release profile suggests that Cur-loaded CS-coated Fe_3O_4 is promising in drug delivery carriers in cancer therapy.

Acknowledgments

References

[1] Chen W, Shen H B, Li X Y, Jia N Q and Xu J M 2006 *Appl. Surf. Sci.* **253** 1762

[2] Shen H B, Long D H, Zhu L Z, Li X Y, Dong Y M, Jia N Q, Zhou H Q, Xin X and Sun Y 2006 *Biophys. Chem.* **122** 1

[3] Liu X, Xing J, Guan Y, Shan G and Liu H 2004 *Colloids Surf. A* **238** 127

[4] Laurent S, Forge D, Port M, Roch A, Robic C, Vander E L and Muller R N 2008 *Chem. Rev.* **108** 2064

[5] Yoon T J, Kim J S, Kim B G, Yu K N, Cho M H and Lee J K 2005 *Angew. Chem. Int. Ed.* **44** 1068

[6] Sundar S, Mariappan R and Piraman S 2014 *Powder Technol.* **266** 321

[7] Mashhadizadeh M H and Diva M A 2012 *J. Nanomed. Nanotechol.* **3** 4

[8] Yao Y, Miao S, Yu S, Ma L, Sun H and Wang S 2012 *J. Colloid Interface Sci.* **379** 20

[9] Peng H, Hu C, Hu J, Tian X and Wu T 2016 *Microporous and Mesoporous Mater.* **226** 140

[10] Ak T and Gülcin I 2008 *Chem. Biol. Interact.* **174** 27

[11] Kawamori T, Lubet R, Steele V E, Kelloff G J, Kaskey R B, Rao C V and Reddy B S 1999 *Cancer Res.* **59** 597

[12] Mahady G B, Pendland S L, Yun G and Lu Z Z 2002 *Anticancer Res.* **22** 4179

[13] Aggarwal B B, Sundaram C, Malani N, Ichikawa H, Aggarwal B B, Surh Y J and Shishodia S 2007 *The Molecular Targets and Therapeutic Uses of Curcumin in Health and Disease* (New York: Springer) pp 1–76

[14] Muller R H and Keck C M 2004 *J. Biotechnol.* **113** 151

[15] Tiyaboonchai W, Tungpradit W and Plianbangchang P 2007 *Int. J. Pharm.* **337** 299

[16] Karikar C, Maitra A, Bisht S, Feldmann G, Soni S and Ravi R 2007 *J. Nano Biotechnol.* **5** 3

[17] Muzzarelli R A, Mattioli B M, Pugnaloni A and Biagini G 1999 *Basel.* **87** 251

[18] Crini G, Gimbert F, Robert C, Martel B, Adam O, Crini N M, Giorgi F D and Badot P M 2008 *J. Hazard. Mater.* **153** 96

[19] Hua L L, Cheng J D, Deng H R, Liu Z L and Li X L 2010 *Chem. Eng. J.* **160** 378

[20] Thacharodi D and Panduranga R K 1993 *J. Chem. Technol. Biotechnol.* **58** 177

[21] Thacharodi D and Panduranga R K 1993 *Int. J. Pharm.* **96** 33

[22] Thacharodi D and Panduranga R K 1995 *Biomaterials* **16** 145

[23] Calvo P, Remunan L C, Vila J L and Alonso M J 1997 *J. Appl. Polym. Sci.* **63** 125

[24] Monks A *et al* 1991 *J. National Cancer Institute* **83** 757

[25] Li S, Zhang T, Tang R, Qiu H, Wang C and Zhou Z 2015 *J. Magn. Magn. Mater.* **379** 226

[26] Pati S S, Mahendran V and Philip J 2013 *J. Nanofluids* **2** 94

[27] Zhang S, Zhang Y, Liu J, Xu Q, Xiao H, Wang X, Xu H and Zhou J 2013 *Chem. Eng. J.* **226** 30

[28] Pavia D L, Lampman G M, Kriz G S, James R and Vyvyan J R 2009 *Introduction to Spectroscopy* 4th edn (Brooks/Cole: Cengage Learning) p 50

[29] Venkataraman A, Vijay A, Hiremeth A, Date S K and Kulkarni S D 2001 *Bull. Mater. Sci.* **24** 617

[30] Mohapatra S, Pramanik N, Mukherjee S, Ghosh S and Pramanik K P 2007 *J. Mater. Sci.* **42** 7566

[31] Yavuz C T *et al* 2006 *Science* **314** 964

[32] Zhu L, Ma J, Jia N, Zhao Y and Shen H 2009 *Colloids Surf.* **68** 1

[33] Volgyi G, Baka E, Box K J, Comer J E and Novak K T 2010 *Anal. Chim. Acta* **673** 40

[34] Kayal S and Ramanujan R V 2010 *Mater. Sci. Eng. C* **30** 484

[35] Nigam S, Chandra S, Newgreen D F, Bahadur D and Chen Q 2014 *Langmuir* **30** 1004